Configuration of ammonia on Cu{311}: Infrared spectroscopy and first-principles theory

Krit Sitathani ; Israel Temprano ; Stephen J. Jenkins ✉

Check for updates
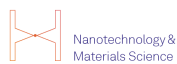
View Online

Export Citation

AIP Publishing

Configuration of ammonia on Cu{311}: Infrared spectroscopy and first-principles theory

View Online   Export Citation   CrossMark

Krit Sitathani,[1] Israel Temprano,[1,2] and Stephen J. Jenkins[1,a]

AFFILIATIONS

[1] Yusuf Hamied Department of Chemistry, University of Cambridge, Lensfield Road, Cambridge CB2 1EW, United Kingdom
[2] CICA - Centro Interdisciplinar de Química e Bioloxía and Departamento de Química, Facultade de Ciencias, Universidade da Coruña, 15071, A Coruña, Spain

[a] Author to whom correspondence should be addressed: sjj24@cam.ac.uk

ABSTRACT

We describe Reflection Absorption Infrared Spectroscopy (RAIRS) and first-principles Density Functional Theory (DFT) studies of ammonia adsorption on the Cu{311} surface. Our experimental results indicate an upright chemisorbed species at low coverages, with at least one additional species accompanying this at higher coverages. Our high-coverage RAIRS data cannot be fully explained by DFT models containing only ammonia or its dissociation products, even allowing for molecular tilt and/or the formation of a bilayer. We therefore also consider urea and formamide as possible products of surface reaction with residual carbon monoxide, but these species are again not fully compatible with our observed spectra. The overlayer composition at high coverages remains mysterious.

I. INTRODUCTION

The surface science of ammonia has been of interest for many decades, not least in the context of its synthesis over heterogeneous iron catalysts (the Haber–Bosch process). Equally important, from the industrial perspective, is the oxidation of ammonia over platinum/rhodium catalysts, which is a key step in the manufacture of nitric acid (the Ostwald process). Moreover, as a decomposition product of urea, ammonia is central to the Selective Catalytic Reduction (SCR) of NO_x gases in the treatment of automotive and power-plant exhaust streams. Practical SCR catalysts include metals, oxides, and zeolites, and again the surface chemistry is key. In recent years, ammonia has also been touted as a possible vector for energy transportation,[1] where one scenario involves exploitation in fuel cells with the anode requiring reactivity somewhere between that of platinum and copper.[2]

In addition to these important current and potential applications, ammonia may be viewed with fundamental interest for the similarities and differences that it displays with respect to that most versatile of solvents, water. Both water and ammonia are classic protic solvents, capable of hydrogen bonding with organic molecules, and the latter has even been proposed as an alternative to the former in hosting exobiological ecosystems on other worlds.[3] On *this* world, meanwhile, although the surface chemistry of water has been subject

to an enormous fundamental research effort,[4–6] that of ammonia has been predominantly of a more applied nature.

Nevertheless, some time ago, one of us reported a series of calculations comparing the adsorption of water and ammonia on Cu{110},[7] concurring with prior experimental studies that indicated near-upright adsorption of ammonia at low coverages giving way increasingly to tilted adsorption in the approach to saturation.[8–10] Whereas the experiments had hitherto been interpreted in terms of a single chemisorbed layer, however, our calculations suggested that high coverages of ammonia resulted in a bilayer, within which only half of the molecules were directly chemisorbed to the surface, the other half attaching to these through hydrogen bonding.[7] Such a structure would be analogous to the bilayers that were once thought to be a common result of water adsorption on metal surfaces. In fact, there is now much evidence to suggest that water partially dissociates on most surfaces,[4–6] yielding a monolayer of mixed H_2O/OH character, and it may be suspected that something similar might be true of ammonia.

In returning to this topic, we now address the Cu{311} surface, which shares distinct structural similarities with the Cu{110} surface but also some important differences of symmetry.[11] On both surfaces, one finds close-packed chains of copper atoms, forming regularly spaced linear steps (see Fig. 1). Notably, the most symmetric primitive unit cell of the {110} surface is rectangular, so that
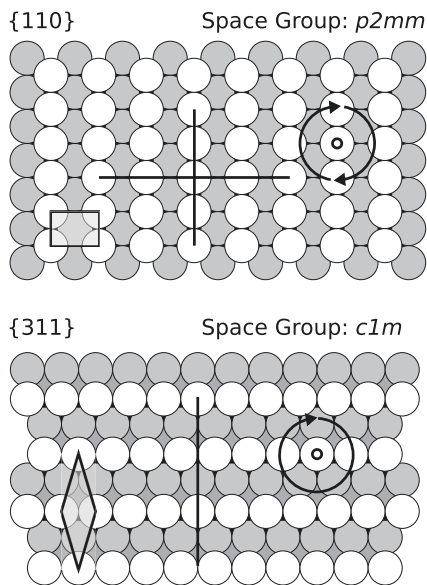
FIG. 1. Comparison of Cu{110} and Cu{311} surfaces. Darker shades indicate deeper layers. In each case, the most symmetric primitive unit cell is marked at the lower left, alongside examples of mirror planes and rotational axes.

atoms from one step line up with those from the next in a perpendicular fashion. On the {311} surface, meanwhile, the most symmetric primitive unit cell is rhombic, and the atoms from one step line up perpendicularly with bridge sites in the next. Owing to the relative disposition of atoms in the second and lower layers, however, the {110} surface displays twofold rotational symmetry but the {311} surface does not. Furthermore, while the {110} surface displays two mirror plane orientations, parallel and perpendicular to its steps, the {311} surface displays only one, perpendicular to its steps. We therefore anticipate that although ammonia adsorption on Cu{311} should show interesting deviations from the situation studied previously on Cu{110}, the two systems may yet shed useful light upon one another.

II. METHODOLOGY

A. Experimental

Experiments were performed inside an ultra-high vacuum chamber, described already elsewhere;[12] here we provide only a brief summary of its main features. The chamber may be conceptually divided into three vertical levels, the uppermost of which accommodated a Leybold Turbovac 151 turbomolecular pump, an ion gauge, and a leak valve for gas dosing. The middle level housed a VG Scienta retractable rear-view Low-Energy Electron Diffraction (LEED) optics, together with a Physical Electronics ion gun and an Ar leak valve for sputtering purposes, and was connected to an Edwards E603 diffusion pump. On the lower level was a Hiden HAL 2 mass spectrometer and KBr viewports for the integration of a Mattson RS2 IR spectrometer intended for Reflection Absorption Infrared Spectroscopy (RAIRS). The gas line connecting to both of the leak valves was pumped by an Edwards E02 diffusion pump. A manipulator (with full $360°$ rotation about the vertical axis) permitted movement of the sample between planes and fine adjustment of horizontal position to optimize the signal during infrared experiments. The typical base pressure for the system was around 6×10^{-11} mbar.

Our Cu{311} single-crystal sample was sourced from MaTeck GmbH and was of 99.9999% purity with dimensions $15 \times 10 \times 1$ mm^3. It was cut to an accuracy of within $1°$ and polished to a roughness of less than 0.03 μm. Mounting to the manipulator was achieved by means of 0.4 mm diameter tantalum wires, located within grooves machined into the top and bottom edges of the sample; these were themselves secured in position by means of 0.125 mm tantalum wires tied through holes drilled into the corners of the sample. The temperature was measured and controlled using a K-type thermocouple (comprising 0.25 mm chromel and alumel wires mounted directly onto the sample) and a Eurotherm PID controller (resistively heating the sample by passing current through the aforementioned 0.4 mm tantalum wires). In conjunction with cooling from a liquid nitrogen cold finger incorporated within the manipulator, the sample temperature could be accurately controlled over the range 95–900 K. The surface was prepared for each experimental run by cycles of Ar$^+$ bombardment (typically at 1 keV) and annealing (typically at 900 K) until a sharp (1×1) LEED pattern was obtained alongside an Auger electron spectrum showing no sign of either carbon or oxygen contamination.

Ammonia was dosed at a pressure of 4×10^{-10} mbar while monitoring its purity via the chamber's mass spectrometer. RAIRS data were acquired, at a resolution of 4 cm^{-1}, by averaging over 400 individual spectra and dividing by a similarly averaged background spectrum obtained from the clean surface immediately before each experiment. Although the spectrometer ought to be capable of operation throughout the 570–4000 cm^{-1} frequency range, in practice we found well-resolved spectral features above the level of noise only within the approximate range 1000–2400 cm^{-1}.

B. Computational

Calculations were performed using the CASTEP code, which implements first-principles density functional theory (DFT) using periodic boundary conditions.[13] Electron–ion interactions were represented by means of ultrasoft pseudopotentials,[14] and wavefunctions were expanded in a plane wave basis up to a kinetic energy cutoff at 340 eV. The exchange–correlation functional was taken in the PBE (Perdew–Burke–Ernzerhof) form.[15] The surface calculations made use of a 12-layer copper slab, within a supercell of length equal to 22 layers in the [311] direction and lateral dimensions consistent with either a $(3, 3; \bar{1}, 1)$ or a $(2, 2; \bar{1}, 1)$ surface unit cell (see Fig. 2). The former was used for calculations involving total surface coverages of 0.17, 0.33, and 0.67 ML, while the latter was used for 0.25, 0.50, and 0.75 ML calculations. Calculations at a total coverage of 1.00 ML were carried out using the smaller cell where this was compatible with the desired coverages of individual species, but the larger cell was used where necessary. The Brillouin zone was sampled on either a $3 \times 3 \times 1$ or a $5 \times 3 \times 1$ Monkhorst–Pack mesh[16] for the larger and smaller cells respectively.

Prior to vibrational calculations, geometries were optimized (while keeping the back seven layers of the slab fixed) to a tolerance of 10^{-5} eV in the total energy and 2×10^{-2} eV Å^{-1} in the maximum force component on any given atom. The resulting relaxed geometries were then used as the input for vibrational calculations carried
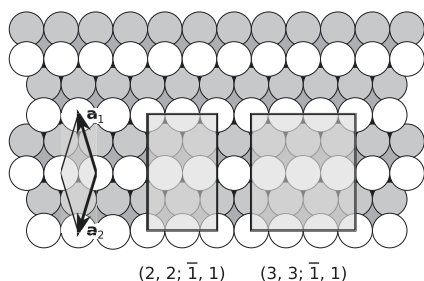
09 August 2024 07:58:12

FIG. 2. Unit cells of the Cu{311} surface.

TABLE I. Experimental[18–23] and calculated frequencies of selected vibrational modes for isolated molecules. Calculations were performed within $10 \times 10 \times 10$ Å^3 cells. In each case, the scaling factor needed to bring the calculated frequency into agreement with the experimental frequency is given.

Molecule	Mode	Expt. (cm^{-1})	Calc. (cm^{-1})	Factor
CO	C–O stretch	2143	2245	0.955
NH$_3$	Umbrella	950	951	0.999
NH$_3$	Deformation	1627	1582	1.028
N$_2$H$_4$	NH$_2$ anti. scissor	1628	1601	1.017
N$_2$H$_4$	NH$_2$ sym. scissor	1642	1640	1.001
CO(NH$_2$)$_2$	NH$_2$ scissor	1590	1576	1.009
CO(NH$_2$)$_2$	C–O stretch	1740	1756	0.991
NH$_2$CHO	C–N stretch	1258	1290	0.975
NH$_2$CHO	CH bend	1390	1432	0.971
NH$_2$CHO	NH$_2$ scissor	1577	1556	1.013
NH$_2$CHO	C–O stretch	1754	1804	0.972

out by the finite-displacement method.[17] In these calculations, only the atoms of the adsorbate were permitted to move, but we have previously tested this restriction in a similar system[12] and found that it has no appreciable effect upon the results.

It is generally accepted that vibrational frequencies obtained from first-principles calculations are often in error by a few percent when compared against experiment. This error may arise due either to the calculated forces not being quite correct or to use of the harmonic approximation in solving the dynamics. It is therefore quite common to apply a scaling factor to calculated mode frequencies, and we follow this pragmatic approach here in order to better compare with experiment. In Table I, we present the experimental frequencies for selected modes of carbon monoxide, ammonia, hydrazine, urea, and formamide, alongside our calculated frequencies and the scaling factors that would transform the latter to the former. These scaling factors have been applied to all corresponding frequencies stated below (unscaled frequencies may be found within the repository listed in the "Data Availability" section).

III. EXPERIMENTAL RESULTS

A. Exposure of clean surface to ammonia

The RAIR spectra obtained during dosing with ammonia at 100 K are displayed in Fig. 3. After an exposure of 0.04 L, the spectrum remains virtually flat, albeit with some features barely above the noise floor in the frequency range 1070–1140 cm^{-1}. A much clearer feature, however, is evident after an exposure of 0.11 L, in the form of a sharp peak at 1120 cm^{-1}, along with a minor disturbance (omitted from the figure) around 2100 cm^{-1} that may relate to the displacement of trace CO from the surface (see the supplementary material). The sharp peak grows as the total exposure increases to 0.18 L, shifting lower in frequency to 1100 cm^{-1}. It is highly likely that this sharp feature corresponds to the symmetric deformation mode (i.e., the umbrella mode) of intact adsorbed NH$_3$, blueshifted from the corresponding gas-phase frequency[18] of 950 cm^{-1}. Such a blueshift has been observed previously upon ammonia adsorption on Cu{110}, both via High-Resolution Electron Energy Loss Spectroscopy[24] (HREELS; in which a peak was initially present at 1150 cm^{-1}, dropping to 1130 cm^{-1} as the exposure increases) and via RAIRS[25] (in which a pair of peaks were seen at 1180 and 1200 cm^{-1}, the former being rapidly swamped by the latter upon increasing exposure). In general terms, the blueshift most likely arises due to electronic changes in each adsorbed molecule as it forms a dative covalent bond with the surface, while the gradual reversal of that blueshift is indicative of a weakening of the adsorbate–substrate bond as the adsorbates are packed ever closer together.

As the exposure continues to increase, the main peak shifts further to lower frequencies, reaching 1078 cm^{-1} by 0.25 L, while broadening and developing a noticeable high-frequency shoulder (its integrated intensity rising, despite a reduction in its maximum excursion from the baseline). After a total exposure of 0.32 L, indeed,
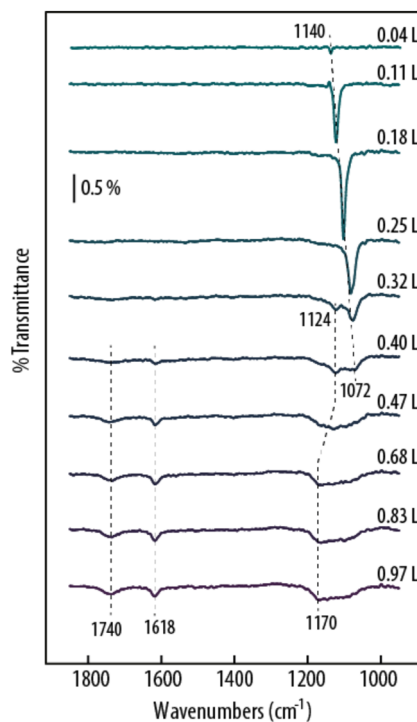

FIG. 3. RAIR spectra obtained during dosing of ammonia onto clean Cu{311} at 100 K.

09 August 2024 07:58:12

the spectrum clearly features two distinct peaks—one, slightly more intense, at 1072 cm^{-1}, and the other at 1124 cm^{-1}. These two peaks remain distinguishable at 0.40 L exposure, though with their relative intensities reversed, but for exposures above 0.47 L, they merge into a single asymmetric peak (skewed toward higher frequencies) covering the approximate range 1050–1200 cm^{-1}. The merging of these umbrella-mode peaks is accompanied by the emergence of two minor peaks at 1618 and 1740 cm^{-1}, which barely shift in frequency as the exposure increases. These two higher-frequency peaks are plausibly in the range expected for the degenerate deformation modes of ammonia, which fall at 1627 cm^{-1} for the gas-phase molecule.[18] The surface selection rule would preclude their observation if ammonia were to adsorb fully upright, but any degree of molecular tilt could render this moot. Quite why there should be *two* such widely separated high-frequency peaks is not, however, readily explicable by a simple model containing only tilted intact adsorbates.

B. Exposure of surfaces pre-dosed with oxygen

In addition to our experiments on the clean surface, we also investigated the adsorption of ammonia onto an oxygen-precovered surface. Specifically, we prepared a surface at room temperature with a low exposure to oxygen, forming an ordered structure whose LEED pattern is consistent with a missing-row reconstruction of the surface and an adatom coverage of 0.5 ML (cf. our previous work on nitric oxide adsorption onto such a surface[12]). We then exposed this prepared surface to ammonia at 100 K, as in the experiments described above. At first, the results are superficially similar, with a fairly sharp peak emerging at 1148 cm^{-1} in the 0.07 L spectrum, shifting gradually to 1119 cm^{-1} in the 0.25 L spectrum (see Fig. 4). These frequencies are, however, somewhat higher than the corresponding frequencies observed upon ammonia adsorption onto the clean surface, suggesting that the presence of pre-adsorbed oxygen enhances the binding of ammonia to the surface. This is unsurprising, since the presence of an electron-withdrawing coadsorbate (oxygen) is likely to be conducive to the binding of a species (ammonia) that adsorbs through the donation of electrons via a dative covalent bond. In addition, the umbrella-mode peak again starts to split into two components at exposures above around 0.25 L, these being just about resolvable at 0.32 L and exhibiting a reversal of relative intensities by 0.40 L. The broad asymmetric peak that eventually formed on the clean surface at higher exposures is present here too, albeit rather more skewed than before and with a definite maximum at 1174 cm^{-1}.

The most striking difference between the spectra obtained on the clean and pre-dosed surface, however, is certainly to be found in relation to the higher-frequency modes that emerge from around 0.40 L exposure. On the clean surface, two peaks are observed, at 1740 and 1618 cm^{-1}, while on the oxygen pre-covered surface, only a single high-frequency peak at 1623 cm^{-1} is ever observed. This would appear to suggest that the two features present within the original spectra arise from two different surface species, the coverage of only one being suppressed by the presence of oxygen. It is just possible, however, that these two peaks correspond to different vibrational modes of the same surface species, in which case the disappearance of one in the presence of oxygen must be explained by reorientation rather than by a change in coverage. For the moment, we maintain an open mind on the subject.
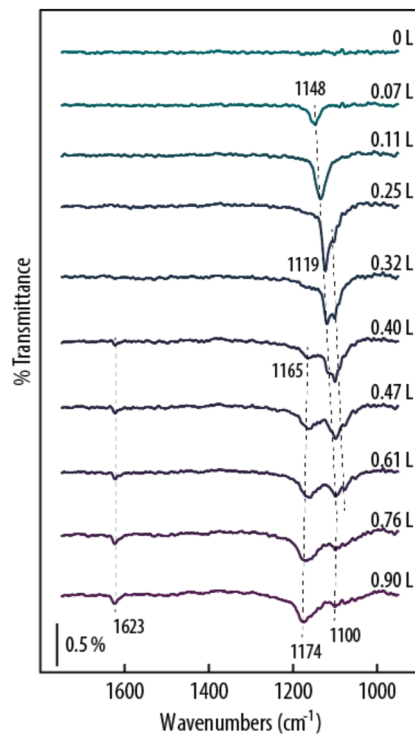

FIG. 4. RAIR spectra obtained during dosing of ammonia onto oxygen pre-dosed Cu{311} at 100 K.

IV. COMPUTATIONAL RESULTS

A. Ammonia and amino

Our calculated adsorption heats (and selected structural parameters) for ammonia (NH$_3$) are summarized in Table II and show a gradual decline from 0.76 eV at 0.17 ML, through 0.67 eV at 0.25 ML, to 0.66 eV at 0.33 ML. In this coverage range, adsorption occurs almost perfectly upright in atop sites (Fig. 5). A very slight molecular tilt starts to emerge at 0.50 ML coverage (0.54 eV), but the mean N–H bond direction for each molecule does not exceed a tilt of 16° from the vertical [Figs. 5 and 6(a)]. The calculated Cu–N bond

TABLE II. Calculated per-molecule adsorption heats, q_a, bond lengths, d, and tilt angles for molecules within pure ammonia overlayers. The "tilt" here refers to the angle between the surface normal and the mean direction of each molecule's three N–H bonds.

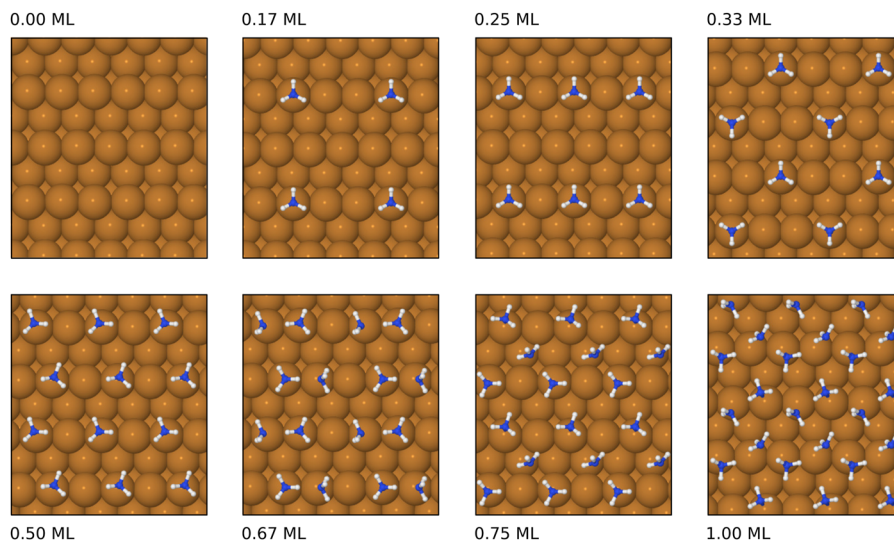| Coverage (ML)	q_a (eV)	d(Cu–N) (Å)	Tilt (°)
0.17	0.76	2.04	3
0.25	0.67	2.07	4
0.33	0.66	2.05/2.05	2/2
0.50	0.54	2.08/2.08	14/16
0.67	0.50	2.04/2.05/3.29/3.29	4/7/84/85
0.75	0.47	2.06/2.09/3.65	10/28/100
1.00	0.39	2.07/2.10/3.44/3.70	29/39/84/88

FIG. 5. Top-down views of calculated ammonia adsorption geometries at a variety of coverages.

lengths, meanwhile, are not very sensitive to coverage, varying only between 2.04 Å and 2.08 Å in the 0.17–0.50 ML range.

Our calculated umbrella mode frequency at 0.17 ML coverage is 1118 cm^{-1} (see Table III), which is very close to our experimentally measured frequency at 0.11 L exposure (1120 cm^{-1}). At a coverage of 0.25 ML, the same mode appears at 1104 cm^{-1}, reproducing the drop in frequency observed in the experiments described above. As

FIG. 6. Oblique views of calculated adsorption geometries for ammonia at (a) 0.50 ML and (b) 0.67 ML. Note the spontaneous formation of a hydrogen-bonded bilayer in the latter case.

the coverage increases further in our calculations, we observe a splitting of this mode due to interactions between neighboring molecules and a continued drop in the mean frequency. At 0.33 ML, we calculate umbrella-mode frequencies of 1094 and 1106 cm^{-1}, while at 0.50 ML we obtain frequencies of 1041 and 1054 cm^{-1}. Although the gradual reversal of the surface-induced blue shift is clear, however, the magnitude of the splitting does not approach the roughly 50 cm^{-1} gap between low- and high-frequency umbrella-mode peaks seen in our RAIRS data at 0.32 L. It appears, therefore, that the mid-range exposures of our experiment probably correspond to surface coverages in excess of 0.50 Ml.

Continuing with calculations involving only NH$_3$ species, we find that all coverages above 0.50 ML result in a bilayer structure [Figs. 5 and 6(b)]. That is, some of the adsorbates remain affixed firmly to the surface, but others float some distance above the surface and remain tethered only by hydrogen bonds to their chemisorbed neighbors. The calculated adsorption heats for the most stable configurations found at each coverage continue to decline, from 0.50 eV at 0.67 ML, through 0.47 eV at 0.75 ML, to 0.39 eV at 1.00 ML.

In the most favorable 0.67 ML structure, half of the adsorbed NH$_3$ molecules display near-vertical orientations (mean N–H bond directions lying within 7° of the surface normal) with Cu–N bond lengths around 2.04 Å, while the other half are tilted such that the mean N–H bond direction for each moiety lies at around 84° from the surface normal. The first- and second-layer molecules bind to each other through hydrogen bonds in a one-to-one fashion, with the nitrogen atoms of the former species acting as donors and those of the latter acting as acceptors. The NH···N length is found to be 2.02 Å. Based on an empirical scaling relationship between hydrogen bond length and strength,[26] we estimate that each such hydrogen bond contributes ~0.25 eV to the overall binding in this configuration.

Turning to the most favorable 0.75 ML structure, we find that two-thirds of the adsorbed NH$_3$ molecules are bound directly to
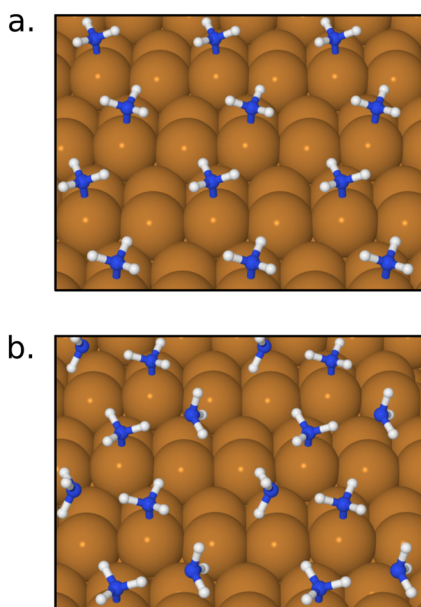
TABLE III. Calculated vibrational frequencies of the umbrella and degenerate deformation modes (v_2 and v_4, respectively) in pure ammonia overlayers. The symmetric and degenerate stretch modes (v_1 and v_3, respectively) lie above 3200 cm^{-1} and are not tabulated.

Coverage (ML)	v_2 (cm^{-1})	v_4 (cm^{-1})
0.17	1118	1605/1646
0.25	1104	1581/1641
0.33	1094/1106	1618/1636/1648/1669
0.50	1041/1054	1605/1608/1620/1631
0.67	1026/1027/1149/1164	1598/1599/1617/1628/1635/1653/1667/1669
0.75	986/1040/1152	1610/1624/1626/1641/1659/1692
1.00	946/999/1068/1135	1598/1599/1629/1634/1647/1662/1671/1695

the surface, but their orientation is a little less vertical than in the case described immediately above (with mean N–H bond directions lying at either 10° or 16° from the surface normal). The Cu–N bond lengths for these chemisorbed moieties are calculated as either 2.06 or 2.09 Å, with the more nearly vertical of them displaying the slightly shorter bond and forming one-to-one hydrogen bonds with molecules in the second layer (the latter tilted by 100° from the surface normal). Once again, the nitrogen atoms of the first-layer molecules function as hydrogen-bond donors, while those of the second-layer function as acceptors. The NH···N length in this instance is calculated to be 1.93 Å, suggesting that the corresponding hydrogen bonds may be very slightly stronger here than those found at 0.67 ML. Half of the chemisorbed molecules (specifically the more tilted ones) are not involved in hydrogen bonding at all.

As for the most favorable of our 1.00 ML structures, here we find half of the adsorbed NH$_3$ molecules binding directly to the surface, with the remainder attached only via hydrogen bonds. In this instance, all the chemisorbed moieties are quite highly tilted (with mean N–H bond directions lying at either 29° or 39° from the surface normal) and their Cu–N bond lengths are a little longer than before, at 2.07 and 2.10 Å, respectively. The second-layer molecules, meanwhile, are strongly tilted (by 84° or 88° relative to the surface normal) and form hydrogen bonds in a one-to-one fashion with those in the first layer, with NH···N lengths of either 1.96 or 2.04 Å (the more tilted molecules having the slightly shorter hydrogen bonds and the less tilted the weaker).

Regarding vibrational frequencies, none of the higher-coverage structures detailed above are entirely consistent with the higher exposure experimental results. At 0.67 ML, the umbrella modes of the chemisorbed molecules are calculated at 1149 and 1164 cm^{-1}—both too high and too close together to match our RAIRS data. The corresponding modes at 0.75 ML are calculated at 1040 and 1152 cm^{-1}—too far apart for any of our spectra in which distinct peaks are observed. Only at 1.00 ML do we find modes, at 1059 and 1135 cm^{-1}, that could be said to correlate with experiment (cf. modes at 1075 and 1124 cm^{-1} found in our RAIRS data at 0.32 L exposure). At all three coverages, we also calculate second-layer umbrella mode frequencies in the range 946–1027 cm^{-1}, but in light of the molecular orientations involved, it seems likely that these would be only weakly observable in experiment, if at all. Most problematically, however, the experimentally observed modes at around 1618 and 1740 cm^{-1} cannot adequately be explained by the

calculations described thus far. At coverages up to 0.33 ML, deformation modes of NH$_3$ are calculated at frequencies in the range 1581–1669 cm^{-1} but ought not to be experimentally observable due to the upright molecular geometry. In the 0.50 ML structure, the molecular tilt might permit observation of such modes, but the range of calculated frequencies spans only 1605–1631 cm^{-1} at this coverage. For our higher-coverage bilayer structures, meanwhile, the range of frequencies for such modes expands again, spanning 1598–1695 cm^{-1}, but even this breadth cannot match the 122 cm^{-1} separation between the two peaks seen in RAIRS. Moreover, there are many calculated frequencies between the two extrema in each high-coverage model, which would be inconsistent with the two rather distinct peaks of the experiment, even leaving aside the fact that none of our calculated deformation modes lies within 45 cm^{-1} of the higher of the two experimental peaks.

Regretfully, therefore, we reach the conclusion that models involving only intact NH$_3$ molecules seem incapable of mimicking our experimental data. Accordingly, we next consider models in which a degree of dissociation may have occurred. Clearly, we do not expect bands from either adatoms (N) or imidogen moieties (NH) to be found in the frequency range covered by our RAIRS experiments, but the scissor mode of adsorbed amino moieties (NH$_2$) might conceivably lie there or thereabouts. Accordingly, we have performed calculations for this species at 0.17 ML coverage in the bridge sites of the surface steps (Fig. 7). Attempts to converge a model in which adsorption occurs on an atop site simply resulted in migration of the adsorbed moiety into a neighboring bridge site. Our favored geometry is rather symmetric, with each molecule binding via two Cu–N bonds of length 1.93 Å and virtually no tilt of the mean N–H bond direction relative to the surface normal. Since it is not particularly meaningful to report an adsorption heat relative to the gas-phase amino radical or anion, we instead calculate that creation of two adsorbed amino moieties from two gas-phase ammonia molecules, accompanied by the desorption of a single gas-phase hydrogen molecule, would release 0.44 eV per adsorbed moiety. The –NH$_2$ scissor mode is calculated to have an unscaled frequency of 1463 cm^{-1} (no higher than about 1520 cm^{-1} after any reasonable scaling) and no other modes fall within the range explored by our experiments. Once again, this model fails to account for the modes seen in RAIRS and, indeed, features a distinct vibration that was certainly not seen in our experiments.
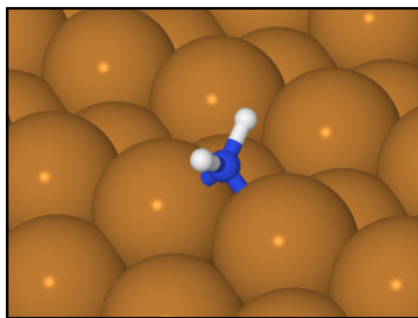
FIG. 7. Calculated adsorption geometry of an amino moiety, binding in a bridge site.

FIG. 8. Calculated adsorption geometries of hydrazine, binding either (a) through a single nitrogen atom or (b) through both of its nitrogen atoms.

B. Ammonium and hydrazine

Having thus exhausted all options afforded by models based only upon NH_3 and its potential dissociation products, we turn next to the possibility that surface species may be formed either by redistributing hydrogen atoms between adsorbates or by forming N–N bonds. One of the more outlandish models considered, for example, was initiated with 0.33 ML NH_4 moieties placed above a surface hosting 0.33 ML chemisorbed NH_3 (in atop sites) and 0.33 ML chemisorbed NH_2 (in bridge sites). In this instance, it might be hoped that ammonium would acquire a positive net charge, binding ionically with a balancing net negative charge induced on the metal surface below. Perhaps unsurprisingly, however, the system reverted to a structure similar to our previously described 1.00 ML NH_3 model, once atoms were permitted to relax (i.e., spontaneous synproportionation occurred). We therefore conclude that NH_4 is not a viable species on the copper surface, consoling ourselves with the thought that it would probably not have exhibited any surface-active infrared modes within the 1600–1750 cm^{-1} range anyway.[27]

In the event that N–N bonds were to be formed on the surface, we believe the most likely product to be hydrazine (N_2H_4) and have therefore performed calculations based upon two possible modes of adsorption (at 0.17 ML coverage). When binding through just one of its nitrogen atoms [placed in an atop site at a surface step, see Fig. 8(a)] we obtain an adsorption heat of 0.72 eV relative to the gas-phase molecule. For reference, our calculations indicate that creation of an adsorbed hydrazine molecule from a gas-phase nitrogen molecule and two gas-phase hydrogen molecules would be exothermic to the tune of 1.72 eV. The Cu–N bond length is 2.02 Å (quite comparable to those formed with adsorbed NH_3) and the N–N bond contracts very slightly to 1.46 Å from a gas-phase length of 1.47 Å. Once again, however, few plausible vibrational modes present themselves in or near the 1600–1750 cm^{-1} range, the closest being symmetric and antisymmetric –NH_2 scissor modes, at 1605 and 1561 cm^{-1} respectively; these modes, moreover, involve almost purely in-plane motion and hence are likely surface-inactive with respect to infrared experiments.

When binding, instead, through both of its nitrogen atoms [Fig. 8(b)] with a calculated adsorption heat of 0.84 eV, the Cu–N bond lengths are both about 2.05 Å, while the N–N bond is again 1.46 Å in length. The calculate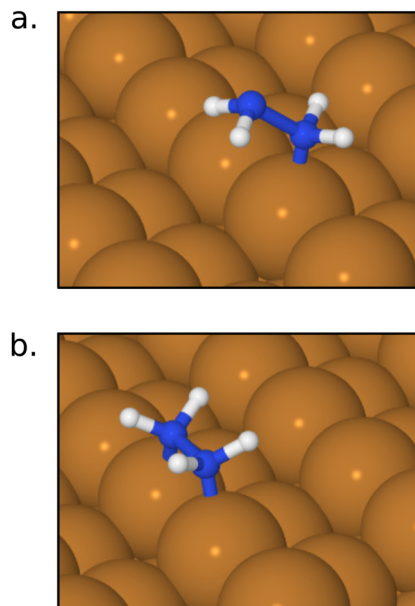d heat of adsorption relative to a stoichiometric set of gas-phase nitrogen and hydrogen molecules is increased to 1.84 eV. The highest-frequency vibrations outside of the stretching region are, as before, symmetric and antisymmetric –NH_2 scissor modes, this time at 1577 and 1560 cm^{-1} respectively. The former of these ought to be surface-active for infrared, but no corresponding peak is seen in RAIRS. There are, meanwhile, no modes at all within the crucial 1600–1750 cm^{-1} window.

C. Carbon monoxide, formamide, and urea

Finally, we address the possible role of surface contamination in giving rise to the two mystery peaks at 1618 and 1740 cm^{-1}, whether directly or after reaction with adsorbed ammonia. In this connection, carbon monoxide (CO) would appear to be the only plausible culprit. We know from our RAIR spectra that a small amount of CO is likely displaced from its preferred adsorption site at the start of our experiments, indicated by the development of a small inverted feature around 2100 cm^{-1} at 0.11 L exposure (see the supplementary material). Its frequency is consistent with expectations for the stretch mode of CO when bound to an atop site on the surface step [Fig. 9(a)]. At the same time, a broad non-inverted feature develops at around 2000 cm^{-1}, suggesting that the atop site may initially be merely modified, rather than prohibited, but this non-inverted feature vanishes entirely at exposures exceeding 0.25 L, while the inverted feature remains constant. It is likely, therefore, that the displaced CO is eventually desorbed rather than simply adsorbed elsewhere. Since the two peaks observed within the 1600–1750 cm^{-1} range emerge only once the exposure exceeds about 0.40 L and, indeed, are not fully developed until after an exposure of at least 0.47 L, it is hard to see how adsorbed CO could be implicated in their origin without giving rise to new inverted peaks (or accentuating existing ones) in the higher-frequency region of the spectrum.
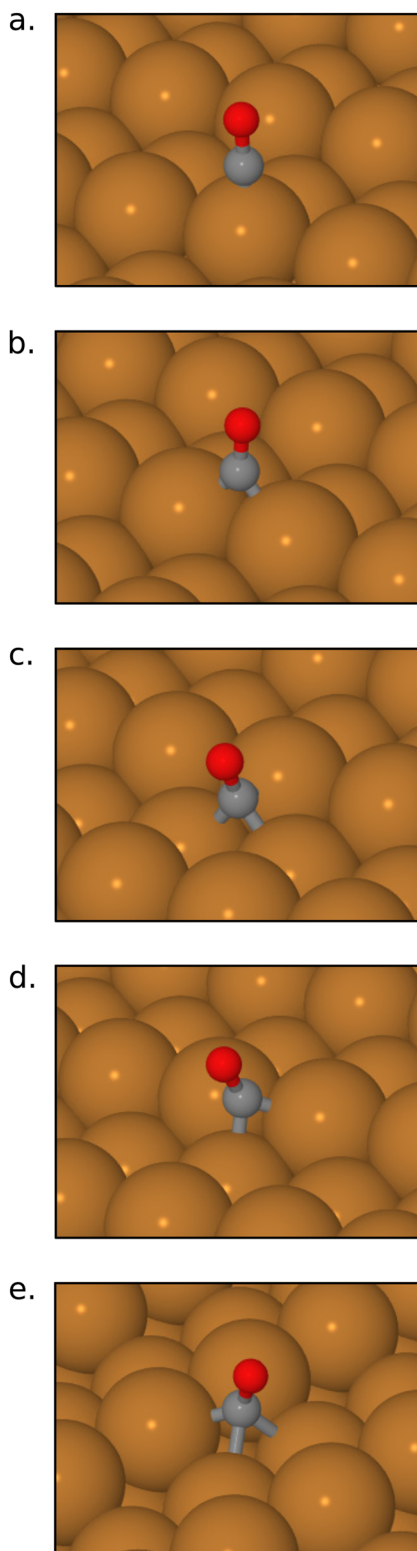
FIG. 9. Calculated adsorption geometries of carbon monoxide, binding through its carbon atom.

Nevertheless, we report, for completeness, on a few candidate species that could be formed.

First, we focus on CO itself, which might conceivably be forced to occupy a high-coordination adsorption site at elevated coverages of ammonia. In a bridge site on the surface step [Fig. 9(b)], we calculated a C–O stretch frequency of 1907 cm^{-1}, which is clearly too high to account for either of our mystery peaks. Meanwhile, within the trough, we identify two distinct threefold hollow sites [Figs. 9(c) and 9(d)] and a fourfold hollow site [Fig. 9(e)]. These give rise to C–O stretch modes at 1797, 1769, and 1708 cm^{-1}, respectively, and it is just about arguable that one or other of the latter two could be reconciled with the observed mode at 1740 cm^{-1}. The observed mode at 1618 cm^{-1} clearly cannot be explained in this way, however, and we reiterate the absence of evidence for further displacement of CO from its preferred adsorption site at exposures in the necessary range.

Turning to the possibility of a reaction between ammonia and carbon monoxide, two species present themselves as conceivable products, one being formamide (NH_2CHO) and the other being urea [$CO(NH_2)_2$]. Both may be produced industrially by the carbonylation of ammonia over suitable catalysts, though the present combination of low temperature and pressure with a rather unreactive metal must give us pause for thought here. It is beyond the scope of the present work to search for transition states linking the proposed reactants and products, but in each case at least one N–H bond would need to be broken (as would also have been the case in forming hydrazine or an amino moiety on the surface) and this is likely to prove prohibitive under cryogenic conditions.

Starting with urea, we assumed an adsorption geometry (at 0.17 ML coverage) in which its two nitrogen atoms bind at neighboring atop sites along a single surface step (Fig. 10). In this model, the Cu–N bonds attain a length of 2.21 Å, which is 5%–10% longer than the typical Cu–N bonds formed upon ammonia or hydrazine adsorption (see above). The C–N and C–O bond lengths are 1.40 and 1.22 Å respectively, compared with 1.37 and 1.23 Å calculated by us for the gas-phase molecule. In this geometry, the adsorption heat relative to gas-phase urea is 0.48 eV, which translates to a release of 1.62 eV when forming the adsorbed species from a gas-phase carbon monoxide molecule and two gas-phase ammonia molecules (eliminating a gas-phase hydrogen molecule). The only vibrational mode that need trouble us is the C–O stretch, for which we calculate a frequency of 1811 cm^{-1} in our favored adsorption
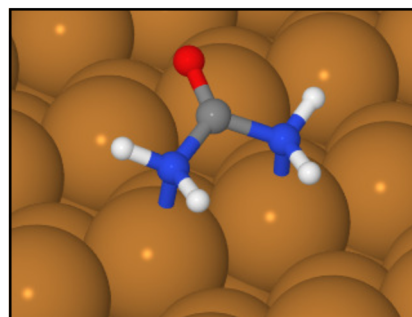

FIG. 10. Calculated adsorption geometry of urea, binding through both of its nitrogen atoms.

geometry. This is clearly rather too high to explain either of the RAIRS peaks found in the 1600–1750 cm^{-1} range, although it is just possible that hydrogen-bonding interactions at higher coverages could bring the frequency down a little. The calculated frequencies in the 900–1600 cm^{-1} range, meanwhile, seem unlikely to be surface-active, owing to the orientation of the molecule (i.e., they primarily involve displacements within the surface plane).

Turning, instead, to formamide, we have calculated three stable adsorption geometries at 0.17 ML coverage—one binding to an atop site on the surface step via the molecule's nitrogen atom and another two binding to the same type of site via its oxygen atom. The nitrogen-bound structure [Fig. 11(a)] is less stable, with a calculated adsorption heat of 0.19 eV relative to gas-phase formamide, to be compared against adsorption heats of 0.46 and 0.59 eV calculated for the oxygen-bound structures [Figs. 11(b) and 11(c), respectively]. These heats translate to the release of 1.44, 1.71, and 1.84 eV upon creation of the adsorbed species from gas-phase ammonia and carbon monoxide. In its more-favorable oxygen-bound geometry, the C–O bond is somewhat stretched, at 1.24 Å, compared with its gas-phase length, while the C–N bond is slightly shortened at 1.33 Å and
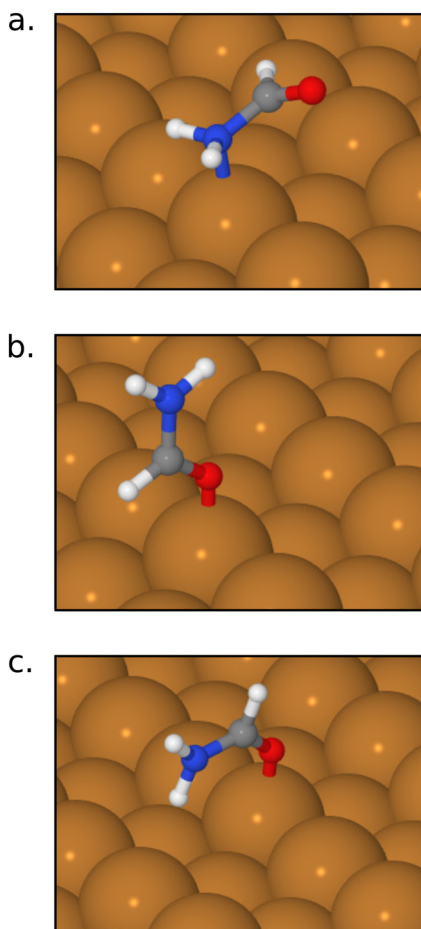

FIG. 11. Calculated adsorption geometries of formamide, binding either (a) through its nitrogen atom or [(b) and (c)] through its oxygen atom.

lies almost parallel to the surface. The Cu–O bond is found to be 2.01 Å in length. In the less stable of the two oxygen-bound geometries, the internal bonds are of much the same lengths, but the Cu–O bond extends slightly to 2.03 Å and the C–N bond lies almost perpendicular to the surface. The frequency of the C–O stretch mode is calculated to be 1680 cm^{-1} in the more stable geometry and 1699 cm^{-1} in the less stable geometry. Both of these seem rather too low to account for the experimentally observed mode at 1740 cm^{-1}, and any hydrogen bonding that might occur at higher coverages is likely only to worsen the agreement.

Meanwhile, in the nitrogen-bound geometry, the C–N and C–O bonds of formamide attain lengths of 1.39 and 1.21 Å, respectively, deviating only slightly from the corresponding lengths of 1.35 and 1.22 Å calculated by us in the gas phase. With a length of 2.26 Å, however, the Cu–N bond is considerably longer than any such bond found among the adsorption systems discussed above. In this case, the C–O stretch mode was calculated at a frequency of 1757 cm^{-1}, which is by far the closest match for the 1740 cm^{-1} experimental peak that we have found among all the species and models considered. It will be appreciated, however, that this close match may be attributed to the lack of interaction between the molecule's oxygen atom and the surface, without which the adsorption heat seems unlikely ever to be competitive.

V. CONCLUSIONS

In summary, observed vibrational modes in the low-exposure regime can quite readily be explained in terms of the (blueshifted) umbrella mode of intact adsorbed ammonia at presumed coverages less than 0.50 ML. In this regime, our first-principles calculations indicate a near-upright geometry for each molecule, consistent with the absence of any RAIRS peaks corresponding to deformation modes. A gradual reversal of the blueshift with increasing coverage is also seen in both experiment and theory, together with a degree of peak-splitting within the 1050–1200 cm^{-1} range.

At higher ammonia exposures, however, the emergence of two modes at 1618 and 1740 cm^{-1} presents a puzzle. Although the lower-frequency mode might appear consistent with a gas-phase ammonia deformation mode, our calculations for the 0.50–1.00 ML coverage range all result in bilayer structures and multiple vibrational frequencies in this vicinity, inconsistent with an isolated RAIRS peak. The higher-frequency mode, moreover, seems entirely inconsistent with any of our ammonia-only models, while its absence from our experimental spectra in the presence of pre-adsorbed oxygen suggests that it may be associated with an entirely separate origin from that of the lower-frequency mode. Models involving amine, ammonium, hydrazine, and urea all fail to produce vibrational frequencies within the 1700–1800 cm^{-1} range. Only in the case of formamide do we find a plausible candidate, with a calculated C–O stretch frequency of 1757 cm^{-1}, but this corresponds to an unfavorable adsorption geometry in which the molecule binds via its nitrogen atom, distinctly less stable than two oxygen-bound geometries with much less promising vibrational modes. High-coordination carbon monoxide is similarly unpromising, despite plausible modes lying between 1708 and 1797 cm^{-1}, since there is no evidence of any displacement from lower-coordination sites within the relevant exposure range.

Finally, therefore, we are forced to conclude that the identity of at least one surface species, giving rise to the 1740 cm^{-1} mode,

remains elusive, although we believe that we have ruled out several apparently plausible (and some less plausible) possible candidates. The mode at 1618 cm^{-1}, however, may yet relate to some conformation of adsorbed ammonia that we have thus far failed to consider. At low coverages, the attribution of mid-range spectral features to blueshifted ammonia umbrella modes is pleasingly uncontroversial and reminiscent of the Cu{110} surface, but at high coverages the behavior on Cu{311} clearly diverges in ways that we have not yet fully resolved.

SUPPLEMENTARY MATERIAL

Spectra showing the 1900–2200 cm^{-1} frequency range, relevant to gauging carbon monoxide contamination, are provided in the supplementary material.

ACKNOWLEDGMENTS

AUTHOR DECLARATIONS

Conflict of Interest

The authors have no conflicts to disclose.

Author Contributions

K.S. was responsible for carrying out the experiments, under the supervision of I.T. and S.J.J. This paper was mainly written by S.J.J., with significant contributions from K.S. and I.T.

Krit Sitathani: Conceptualization (equal); Investigation (equal); Writing – original draft (supporting); Writing – review & editing (supporting). **Israel Temprano**: Conceptualization (equal); Investigation (supporting); Project administration (equal); Supervision (equal); Writing – original draft (supporting); Writing – review & editing (supporting). **Stephen J. Jenkins**: Conceptualization (equal); Investigation (equal); Project administration (equal); Supervision (equal); Writing – original draft (lead); Writing – review & editing (lead).

DATA AVAILABILITY

Additional material supporting the findings of this study is available within the University of Cambridge Data Repository at https://doi.org/10.17863/CAM.105421.

REFERENCES

[1] N. Salmon and R. Bañares-Alcántara, "Green ammonia as a spatial energy vector: A review," Sustainable Energy Fuels **5**, 2814–2839 (2021).

[2] G. Jeerh, M. Zhang, and S. Tao, "Recent progress in ammonia fuel cells and their potential applications," J. Mater. Chem. A **9**, 727–752 (2021).

[3] J. Griffin, "A study of life-type processes in liquid ammonia," Ph.D. thesis, University of Huddersfield, 2015.

[4] A. Hodgson and S. Haq, "Water adsorption and the wetting of metal surfaces," Surf. Sci. Rep. **64**, 381–451 (2009).

[5] J. Carrasco, A. Hodgson, and A. Michaelides, "A molecular perspective of water at metal interfaces," Nat. Mater. **11**, 667–674 (2012).

[6] T. K. Shimizu, S. Maier, A. Verdaguer, J.-J. Velasco-Velez, and M. Salmeron, "Water at surfaces and interfaces: From molecules to ice and bulk liquid," Prog. Surf. Sci. **93**, 87–107 (2018).

[7] G. Jones and S. J. Jenkins, "Water and ammonia on Cu{110}: Comparative structure and bonding," Phys. Chem. Chem. Phys. **15**, 4785–4798 (2013).

[8] N. A. Booth, R. Davis, R. Toomes, D. P. Woodruff, C. Hirschmugl, K. M. Schindler, O. Schaff, V. Fernandez, A. Theobald, P. Hofmann, R. Lindsay, T. Gießel, P. Baumgärtel, and A. Bradshaw, "Structure determination of ammonia on Cu(110)—A low-symmetry adsorption site," Surf. Sci. **387**, 152–159 (1997).

[9] D. Mocuta, J. Ahner, and J. T. Yates, "Adsorption and electron-stimulated dissociation of ammonia on Cu(110): An ESDIAD study," Surf. Sci. **383**, 299–307 (1997).

[10] J. Hasselström, A. Föhlisch, O. Karis, N. Wassdahl, M. Weinelt, A. Nilsson *et al.*, "Ammonia on Cu(110): An angle resolved x-ray spectroscopic and *ab initio* study," J. Chem. Phys. **110**, 4880–4890 (1999).

[11] S. J. Jenkins and S. J. Pratt, "Beyond the surface atlas: A roadmap and gazetteer for surface symmetry and structure," Surf. Sci. Rep. **62**, 373–429 (2007).

[12] K. Sitathani, S. J. Jenkins, and I. T. Temprano, "Partial reduction of NO to N$_2$O on Cu{311}: Role of intermediate N$_2$O$_2$," Catal. Sci. Technol. **12**, 2793–2803 (2022).

[13] S. J. Clark, M. D. Segall, C. J. Pickard, P. J. Hasnip, M. I. J. Probert, K. Refson, and M. C. Payne, "First principles methods using CASTEP," Z. Kristallogr.–Cryst. Mater. **220**, 567–570 (2005).

[14] D. Vanderbilt, "Soft self-consistent pseudopotentials in a generalized eigenvalue formalism," Phys. Rev. B **41**, 7892–7895 (1990).

[15] J. P. Perdew, K. Burke, and M. Ernzerhof, "Generalized gradient approximation made simple," Phys. Rev. Lett. **77**, 3865–3868 (1996).

[16] H. J. Monkhorst and J. D. Pack, "Special points for Brillouin-zone integrations," Phys. Rev. B **13**, 5188–5192 (1976).

[17] K. Refson, P. R. Tulip, and S. J. Clark, "Variational density-functional perturbation theory for dielectrics and lattice dynamics," Phys. Rev. B **73**, 155114 (2006).

[18] T. Shimanouchi, *Tables of Molecular Vibrational Frequencies Consolidated* (National Bureau of Standards, 1972), Vol. I.

[19] J. R. Durig, M. G. Griffin, and R. W. MacNamee, "Raman spectra of gases. XV: Hydrazine and hydrazine-d$_4$," J. Raman Spectrosc. **3**, 133–141 (1975).

[20] K. P. Huber and G. Herzberg, *Molecular Spectra and Molecular Structure IV. Constants of Diatomic Molecules* (Van Nostrand Reinhold, 1979).

[21] Y. Sugawara, Y. Hamada, and M. Tsuboi, "Vibration-rotation spectra of formamides," Bull. Chem. Soc. Jpn. **56**, 1045–1050 (1983).

[22] L. V. Gurvich, I. V. Veyts, and C. B. Alcock, *Thermodynamic Properties of Individual Substances*, 4th ed. (Hemisphere Publishing Corporation, 1992), Vol. I.

[23] A. Vijay and D. N. Sathyanarayana, "*Ab initio* study of the force field, geometry and vibrational assignment of urea," J. Mol. Struct. **295**, 245–258 (1993).

[24] D. Lackey, M. Surman, and D. A. King, "Adsorption of ammonia on Cu{110}," Vacuum **33**, 867–869 (1983).

[25] C.-M. Pradier, A. Adamski, C. Méthivier, and I. Louis-Rose, "Interaction of NH$_2$ and oxygen with Cu(110) investigated by FT-IRAS," J. Mol. Catal. A: Chem. **186**, 193–201 (2002).

[26] G. Jones, S. J. Jenkins, and D. A. King, "Hydrogen bonds at metal surfaces: Universal scaling and quantification of substrate effects," Surf. Sci. **600**, L224–L228 (2006).

[27] M. E. Jacox and W. E. ThompsonGuest researcher National, "Infrared spectrum of the NH$_4$·d$_n^+$ cation trapped in solid neon," Phys. Chem. Chem. Phys. **7**, 768–775 (2005).